An Experimental Study of Parameters Affecting a Heat Pipe Performance

Dr. Hussain H.Ahmad
College of Engineering
University of Mosul

Raqeeb H. Rajab
College of Agriculture and forestry
University of Mosul

Abstract

An experimental test rig was designed and manufactured to investigate the performance of a heat pipe(HP). The heat pipe consists of a stainless steel pipe lined with a three-layer stainless steel mesh wick. The evaporator section of the heat pipe was surrounded by three heaters representing the heat source. The condenser was jacketed with galvanized cylinder to accommodate the cooling water flow. The entire HP was insulated. Different affecting parameters were investigated experimentally in this study including the power input the filling charge of the working fluid(water) represented by a volumetric ratio with respect to evaporator volume and the inclination angle with a horizontal line. All tests were carried out at a pressure around the atmospheric pressure during steady state conditions. The experimental results showed that the conductivity was about (2060) times that of the solid piece of the stainless steel (the material of the HP).A comparison between the present work results with empirical and theoretical correlations of other researchers showed a good agreement.

Key words: heat pipe , wick , filling ratio

<div dir="rtl">

دراسة عملية للعوامل المؤثرة على أداء أنبوب حراري

د.حسين حامد احمد   رقيب حمادي رجب

كلية الهندسة /جامعة الموصل   كلية الزراعةوالغابات/ جامعة الموصل

الخلاصة

تم تصميم الجهاز المختبري وتصنيعه للتحري تجريبياً في أداء الأنبوب الحراري. يتكون الأنبوب الحراري من أنبوب فولاذ مقاوم للصدأ مبطن بفتيلة ذات ثلاث طبقات من (شبكة سلكية من الفولاذ المقاوم للصدأ). مقطع المبخر محاط بثلاثة مسخنات تمثل المصدر الحراري, أما المكثف فتحيطه صفيحة اسطوانية مغلونة يجري خلالها ماء التبريد. تم عزل الأنبوب الحراري كاملاً . في هذه البحث تم التحقق تجريبياً من تأثير عوامل مختلفة تتضمن الطاقة المجهزة للمبخر, كمية شحن السائل التشغيلي(الماء) متمثلة بنسبة حجميه من حجم المبخر وبزوايا ميل متغيره مع المستوى الأفقي تحت ضغط مقارب للضغط الجوي عند حالة الاستقرار. أظهرت النتائج التجريبية أن الموصلية الحرارية هي بحدود (2060) مره بقدر موصلية قطعه صلدة من الفولاذ التي صنع منها الأنبوب الحراري. المقارنة بين نتائج العمل الحالي مع نتائج معادلات عملية ونظرية لباحثين آخرين أظهرت توافقاً جيداً .

</div>

Nomenclature

Symbol	Meaning	Unit
A	AREA	M^2
C_p	Specific heat capacity	$J/kg.°C$
C_{sf}	Constant, determined from experimental data	---
D	Diameter	m
FR	Filling ratio	%
g	Gravitation acceleration	m/s^2
h	Heat transfer coefficient	$W/m^2.°C$
h_{fg}	Latent heat of vaporization	J/kg
HP	Heat pipe	---
K	Permeability	m^2
k	Thermal conductivity	$W/m.°C$
L	Pipe length	m
P	Pressure	N/m^2
P_r	Prandtl number = $\mu \cdot C_p / k$	----
Q	Heat transfer rate	W
q	Heat flux	W/m^2
R	Resistance	m
T	Temperature	°C
W	Power	W
ΔP	Pumping head	N/m^2
μ	Viscosity	$kg/m.s$
ρ	Density	kg/m^3
σ	Surface tension	N/m
β	Angle of inclination	degree
ϕ	Wet angle	degree

Subscripts

a	Adiabatic	ent	Entrainment	o	Outer
av.	Average	eff.	Effective	v	Vapor
bo.	Boiling	exp.	Experimental	vis	Viscous
c	Condenser	in	Inner	s	Sonic
cap.	Capillary	l	Liquid.	w	Wall
e	Evaporator	t	Total	ws	Wick structure

1: Introduction

The heat pipe is a device that efficiently transports heat from one end to another. It utilizes the latent heat of the vaporized working fluid instead of the sensible heat. The two-phase heat transfer mechanism results in heat transfer capabilities from one hundred to several thousand times that of an equivalent well known conductor such as copper[1,7]. The heat pipe operates on a closed two phase cycle. Figure(A) shows a schematic of a typical heat pipe. Inside the heat pipe there is liquid-vapor equilibrium and when the heat is supplied to the evaporator, this equilibrium breaks down as the working fluid evaporates. The vapor, which then has a higher pressure, moves inside the HP to the condenser section where it condenses. Thus, the vapor gives up the latent heat of vaporization and transfers heat from the input to the output end of the heat pipe. The capillary pressure created by the menisci in the wick pumps the condensed fluid back to the evaporator section. Therefore, the heat pipe can continuously transport the latent heat of vaporization from the evaporator to the condenser section. This process will continue as long as there is a sufficient capillary pressure to drive the condensate back to the evaporator. For the last four decades, two-phase passive heat transfer devices like heat pipes were used. A considerable experimental and theoretical works have been done on the application and design modification for improving heat pipes performance. Yahya [1] carried out an experimental study concerned the development of an indirect type of solar cooker using a heat pipe for transporting energy from the focal spot. Frank[2] conducted an experimental investigation of improved injection lances with heat pipe having two wraps of stainless steel mesh as a wick structure in the heat pipe. Kempers et al.[3] carried out an experimental study to determine the effect of the number of mesh layers and amount of working fluid on the heat transfer performance of copper–water heat pipes with screen mesh wicks. Jianlin et al.[4] described a proposed capillary pumped loop(CPL) using the multi-layer copper mesh as the capillary structure in the evaporator. Shwin-Chung et al. [5] in their work presented visualization of the evaporation/boiling process and thermal measurements of operating horizontal transparent heat pipes.

The most obvious pointer to the success of the heat pipe is the wide range of applications where its unique properties have proved to be beneficial. Some of these applications of the heat pipe have played an important role in a variety of engineering heat transfer systems. It would be a difficult task to list all the applications of heat pipes; therefore, only a few important industrial applications are given in this section. In the aerospace industry, heat pipes have been used successfully in controlling the temperature different component. Heat pipes have been applied in cooling different electronics devices. Other applications include cooling of turbine blades, generators, motors. Also heat pipe are used in heat collection from exhaust gases, solar and geothermal energy. In general, heat pipes have advantages over many traditional heat-exchange devices when heat has to be transferred isothermally over relatively short distances, low weight is essential and low maintenance is mandatory[6].

There has been a potential consideration of using heat pipes recently because of the wide range of applications specially in cooling electronic systems. The present work investigates experimentally heat transfer characteristics performance of HP by designing and construction of an experimental test rig studying the affecting parameters. The experimental results of this work were compared with well known theoretical and empirical correlations of Rohsenow and Imura[6,7,13].
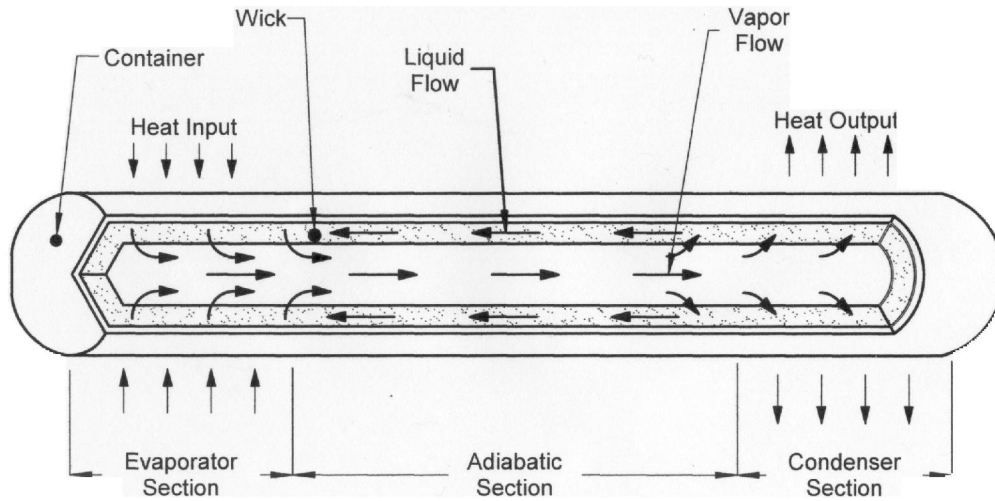
Figure(A):Schematic diagram of the HP and its principles of operation[9].

2: Transport Limitations

The heat input to the heat pipe can be limited to a certain value beyond which the heat

pipe failure or works at low performance. So it is essential for a designer to examine all types of limitations to be sure that it works perfectly at high level of performance.

Limitations of the maximum heat input that may be transported by a heat pipe can be divided into two primary categories: limits that result in heat pipe failure and limits that do not[9]. For the limitations resulting in heat pipe failure, all are characterized by insufficient liquid flow to the evaporator for a given heat input, thus resulting in dry out of the evaporator wick structure. The two categories and basic phenomena for each limit may be summarized as follows:

2.1: Limitations(Failure): limitations include:

2.1.1:Capillary Limit: The ability of a capillary structure to provide the circulation for a given working fluid is called capillary limit or hydrodynamic limit. It occurs when the pumping rate is not sufficient to provide enough liquid to the evaporator section[6].To understand this heat transfer limit, it is essential to know the capillary action and the phenomenon that governs it. For most heat pipes the maximum heat transfer due to the capillary limitation can be expressed as follows[6,10,12].

$$Q_{max,\,cap.} = \left[\frac{\rho_l \sigma_l h_{fg}}{\mu_l}\right]\left[\frac{A_{ws} K}{L_{eff}}\right]\left[\frac{2}{r_{cap}} + (\frac{\rho_l}{\sigma_l})gL_t \cos \beta\right] \qquad (1)$$

Where; L_{eff} is the effective length of the HP $=0.5(L_e+2L_a+L_c)$

2.1.2:Boiling Limit: When the radial heat flux in the evaporator section becomes too high, the liquid in the evaporator wick boils and the wall temperature becomes excessively high. The vapor bubbles that form in the wick prevent the liquid from wetting the pipe wall, causing hot spots.

Severe case of this phenomenon is complete evaporator dry out. This is known as the boiling limit.

An expression for the heat flux beyond which bubble growth will occur can be written as[6,10,12]:

$$Q_{max, \ bo.} = \left(\frac{2\pi L_e \ (k_{eff})_{ws} \ T_v}{h_{fg} \ \rho_v \ \ln(r_i/r_v)} \right) \left(\frac{2\sigma}{r_n} - \Delta P_{cap \ , max} \right) \tag{2}$$

2.1.3:Entrainment Limit: In a heat pipe, liquid and vapor move in opposite direction. A shear force exists at the liquid-vapor interface. High vapor velocity may cause some droplets of liquid to be carried away with the vapor, back to condenser. This inhibits the return of the liquid to the evaporator. A method to determine the entrainment limitation using Weber's number criterion (the Weber number is defined as the ratio of viscous shear force to the surface tension) as follows [6,12].

$$Q_{max, ent.} = A_v h_{fg} \left(\frac{\sigma \rho_v}{2 r_{cap}} \right)^{0.5} \tag{3}$$

2.2:Limitations (Nonfailure):

2.2.1:Sonic Limit: The evaporator and condenser sections of a heat pipe represent a vapor flow channel with mass addition and extraction due to evaporation and condensation, respectively. Sonic limitation is analogous to a converging-diverging nozzle with a constant mass flow rate. The vapor velocity increases along the evaporator and reaches a maximum at the end of the evaporator section[12]. An expression for this limit derived from one dimensional vapor flow theory[6,9,10,14]with a final form:

$$Q_{max, so.} = 0.474 A_v h_{fg} (\rho_v P_v)^{1/2} \tag{4}$$

2.2.2:Viscous Limit: At low operating temperature, the vapor pressure difference between evaporator and condenser regions of a heat pipe may be extremely small. The viscous forces within the vapor region may be dominant over the pressure gradient because of the temperature. In this condition, the pressure gradient may not be sufficient to generate flow and the vapor may stagnate. Mathematically, this limit can be expressed as[6,9,12]

$$Q_{max, vis.} = \frac{A_v r_o^2 h_{fg} \rho_v P_v}{16 \mu_v L_{eff}} \tag{5}$$

2.2.3:Condenser Limit: The heat transfer rate in the condenser section is governed by the coupling of the condenser with the system heat sink. At steady state, the heat rejection rate in the condenser must equal the heat addition rate in the evaporator. Typically, the condenser coupling is either by convection and/or radiation[9].To reach the condenser limit it can be low convective heat transfer coefficients (e.g., natural convection), low surface emissive, or limited surface area. The heat transfer (outlet heat) from the condenser, cooled by water, is determined by:

$$Q_c = \dot{m} C_p (T_o - T_i) = Q_o \tag{6}$$

Additionally, the capillary, viscous, entrainment, and sonic limits are axial heat flux limits, that is, functions of the axial heat transport capacity along the heat pipe. However, the boiling limit is a radial heat flux limit occurring in the evaporator. The maximum theoretical

power input limitations calculated from equations 1,2 ,3,4and 5 are shown in table(1).These values are essential to indicate the maximum input power limit, which were considered in the design of the present experimental rig.

Table(1): Summarize the maximum theoretical power input limitations.

Q_{IN} (W)	$Q_{MAX,BO.}$ (W)	$Q_{MAX,CAP.}$ (W)	$Q_{MAX,ENT.}$ (W)	$Q_{MAX,SO.}$ (W)	$Q_{MAX,VIS.}$ (W)
1500	2396	4629	20429	32639	10986

3: Experimental Apparatus

The heat pipe body , was made from stainless steel pipe with length of (1200)mm, outside and inside diameter of (48)mm and (43)mm respectively. The heat pipe is heated by electrical coils clamped on the evaporator and it is cooled by water flowing through a jacket along the condenser. Between the evaporator and condenser there is adiabatic zone. The pipe lined with capillary structure of three layer stainless steel screen wire mesh (2×150 and 1×80).

Twenty two calibrated thermocouples (chromel – alumel ; type K) were used in temperature measurement that distributed along and around the entire length of HP. The thermocouples were embedded, along (110)mm equally spaced, in 1.5mm depth grooves machined on the outer surface of the wall. An electronic reader [model:E5C4,range (0 - 400 ºC), type K],with a resolution of (1ºC) was used to display temperature readings directly. The sheaths of the thermocouples were fully insulated.

As shown schematically in figure (B) the evaporator has a length of (360)mm, heated electrically by three clamped heaters. The end of the evaporator was sealed with a cup equipped with a drain valve, and another valve connected to a glass level measurement to determine the working fluid level in the evaporator. In order to measure the average temperature of the evaporator, eight thermocouples were distributed along and around it.

The condenser has a length of (500)mm, cooled by water flowing through a jacket of(120)mm diameter and (510)mm in length, fabricated from a galvanized plate of (2)mm thickness. To measure the average temperature of the condenser, six equally spaced thermocouples distributed along and around the external circumference of the condenser.

The segment between the evaporator and the condenser is normally referred to as the adiabatic section with a length of (340)mm. To measure the average temperature of the adiabatic section, six thermocouples were distributed along and around it.

The power was supplied to the evaporator by electrical coil heaters (500 Watt each) mounted between two layers of mica . The length of each heater is (100)mm and (4)mm thickness. The heaters were fixed tightly around the outside surface of the evaporator to insure good contact with its outer surface. surrounding by (20)mm thick asbestos. In order to reduce heat losses to the surrounding, the whole length of the heat pipe was wrapped by two layers of fiber glass.

An accurate wattmeter covering the anticipated power range, and a variac were incorporated in the heater electrical circuit to record the exact power supplied, as shown in figure(B).The heat output of the condenser was calculated from the amount of cooling water flowing through the condenser and the temperature difference between the inlet and outlet of cooling water. The water mass flow rate was measured by an accurate rotameter.
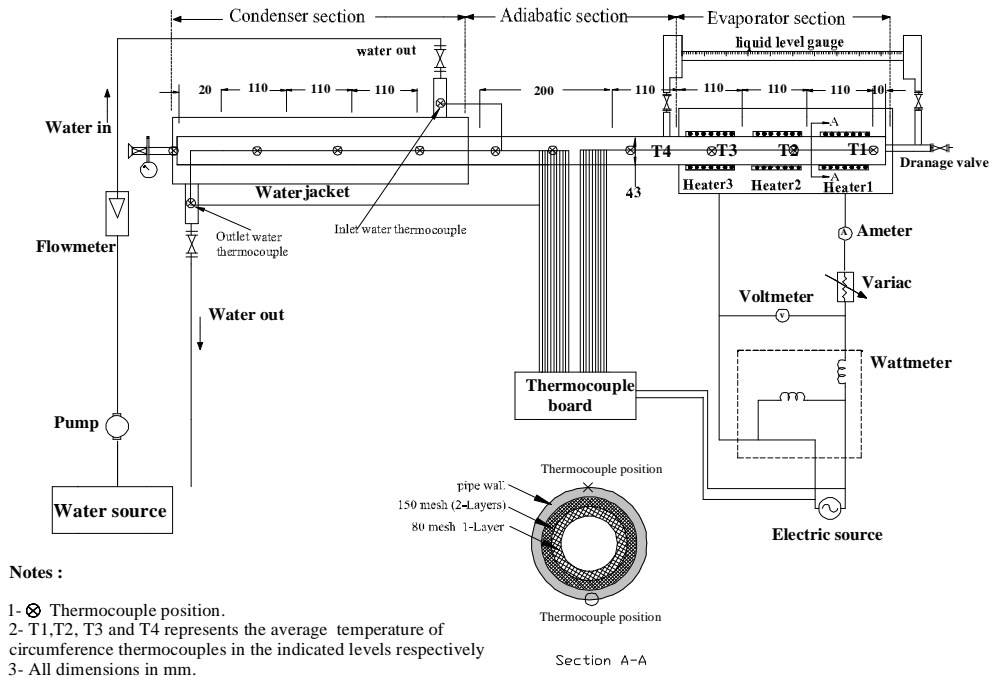
Figure(B):The experimental test rig diagram showing locations heaters and thermocouples.

4: Result and Discussion
4.1: Start-up operation
Heat pipe operation processes can be divided into three stages : start-up, transition and steady state. The first stage is startup, and HP startup tests are the most critical for evaluating the capillary evaporator reliability[10].The startup time for low heat loads was longer than that for high heat loads. Figure(1) shows the distribution of temperatures of the evaporator surface at different positions and different time intervals when the heat input to the evaporator was 250W and 1500W, the filling ratio was 75%,and angle of orientation was 90°. At low heat load, the startup time takes about 90 min. to complete, while at high heat load the startup time takes about 60 min.. The startup HP needs some time in order to discharge excess liquid and to stabilize the vapor-liquid interface at the top. At the end of the startup process a transition stage begins, and one can observe the scattering in wall temperatures. The steady process is indicated by the stability of the HP pressure at nearly one atmosphere, and the stability of the wall temperatures.

4.2:Heat Pipe Thermal Resistance and Thermal Conductivity:
Mathematical correlations were used to calculate each thermal resistance. The effective thermal conductivity of the heat pipe is defined as the heat transfer rate divided by the temperature difference between the heat source and heat sink. Under normal operating conditions, the total thermal resistance is relatively small according to the low value of the difference between the temperature of heat source in the evaporator and the heat sink in the condenser represented by (ΔT). Thus, the effective thermal conductivity in a heat pipe can be very large[14]. The quantity

103

L/Ak is equivalent to a thermal resistance R of the HP wall against the flow of heat by conduction; $R = L/A.k$ .The reciprocal of the thermal resistance $1/R$, refers to the thermal conductance ($A.k/L$)[15]
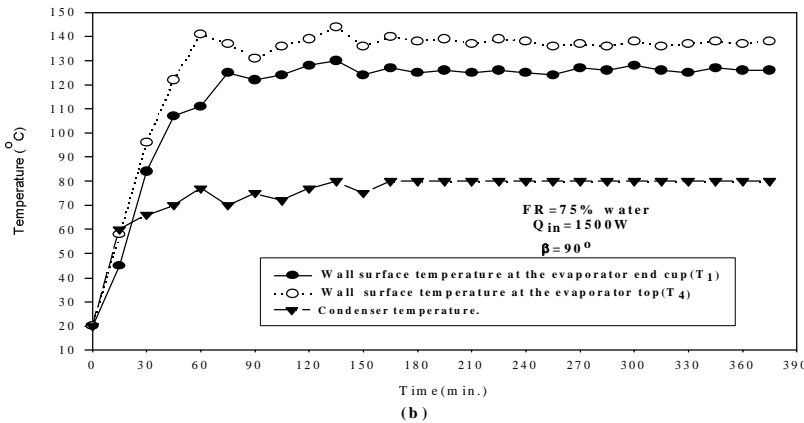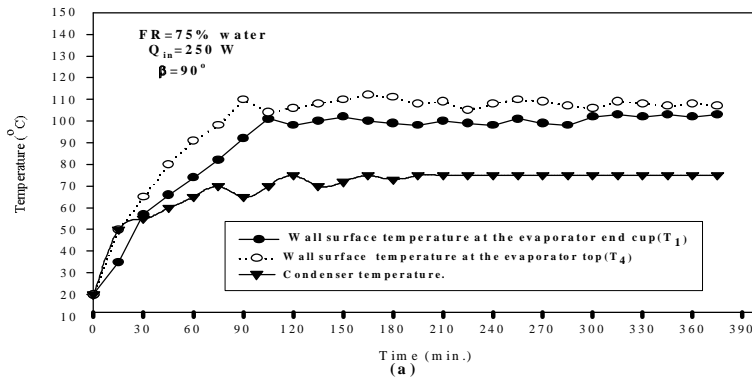
$$R_t = \frac{\Delta T}{Q_{av.}}$$

$$\because Q_{av.} = \frac{k \times A}{L} \cdot \Delta T$$

$$\therefore (k_{eff})_{HP} = \frac{L_t}{R_t \, A_t} \tag{7}$$

From equation (7) k_{eff} was found to be (35638 W/m.$^{\circ}$C   )

Compared to the conductivity of sold stainless steel (16.4   W/m.$^{\circ}$C),the maximum thermal conductivity ($k_{eff}/k_{st.st.}$) = 2060

Figure(1):Temperature variation of the HP wall surface during the startup process for water charge and different heat input (Refer to Fig.B).

4.3: Effects of Filling Ratio and Power input on the temperature distribution

The amount of liquid charge is governed by two considerations; too small quantity can lead to dry out, while an excess of liquid can lead to a condition where an amount of the liquid being carried up to the condenser causing a blockage of surface preventing condensation in the condenser. In this study the filling ratio of the working fluid in the HP is defined as the ratio of the working fluid volume to the entire volume of the evaporator,(i.e. fluid charge rated to the total volume of the evaporator). Three different filling ratio(25%,50% and 75%)were considered. The inventory volume must be able to accommodate at least the liquid volume swing and density changes between the hot section and the cold section of the HP [5]and it must be enough to saturate the wick. At any operating mode of the heat pipe, both liquid and vapor phases have to coexist in it. Hence, it is worthy to study the filling ratio effect on the heat pipe performance. Figures (2)and(3) show the variation of the temperature along the heat pipe for three different filling ratios with heating load rates of 250 and 1500 W at a given inclination angle. The temperature starts to increase along the evaporator to a maximum value and decreases until the adiabatic zone.
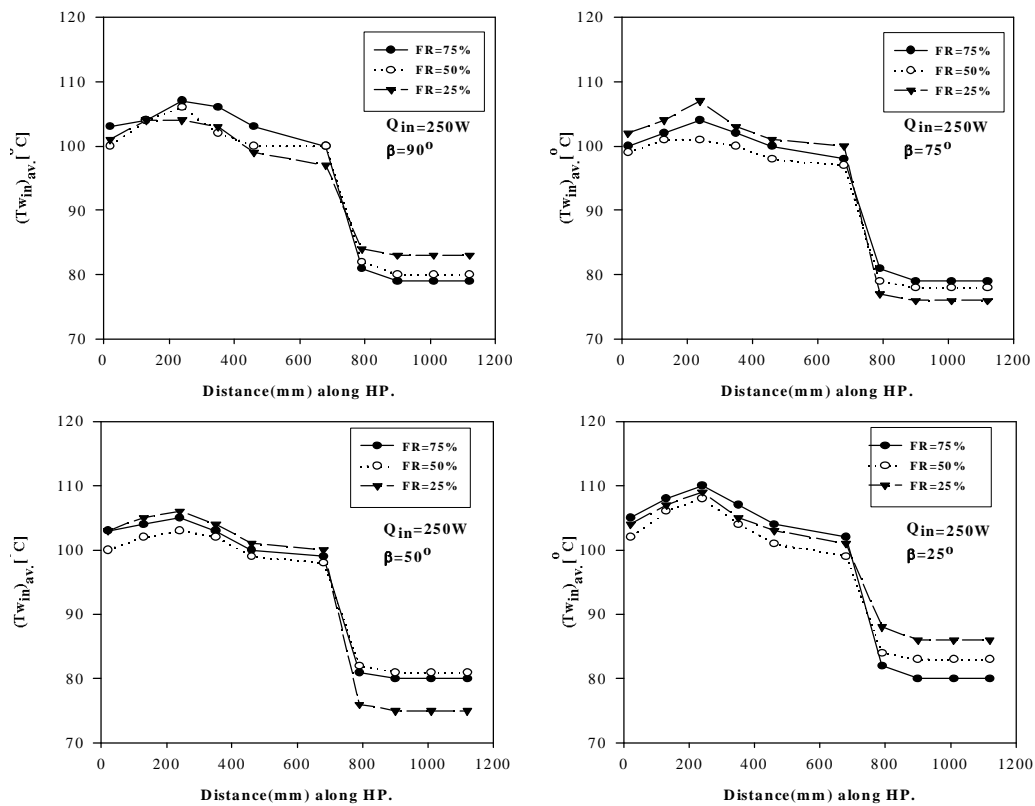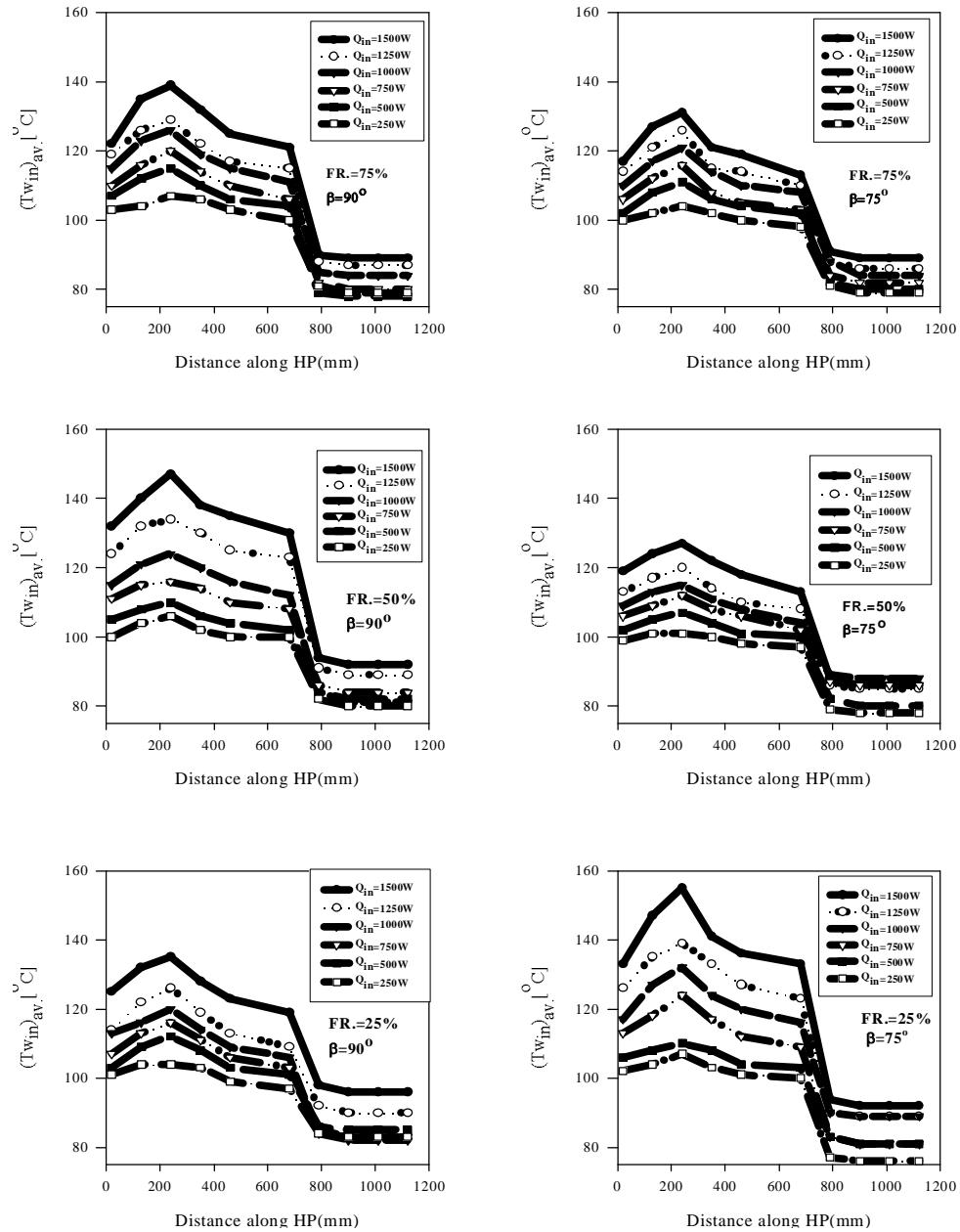
Figure(2):Variation of average wall temperature along the HP with different water filling ratios for different inclination angles.

105

Then the temperature decreases sharply(due to cooling) when vapor enters the condenser and stays constant with very little variation. At all heat transfer rates, however, the temperature at the end of the evaporator is always lower than the other evaporator temperatures. The reason of this lower value is not clear[7], but probably due to that the end of the evaporator was not completely insulated, resulting in a heat leak from this point. Also from the figures above, in general, the temperature is the highest when the filling ratio is(25%). At all input powers figures(4)and(5) show that as the power input increases the temperature also increases regardless of the filling ratio at a given inclination angle. The increase of the temperature along the evaporator section of the heat pipe is due to the phase change of the working fluid from liquid in the end cup of the evaporator to mixture (vapor and liquid) and then to single phase (vapor) where the maximum temperature difference occurs, due to returned liquid from condenser to the evaporator (because of the capillary effect) the temperature decrease again.
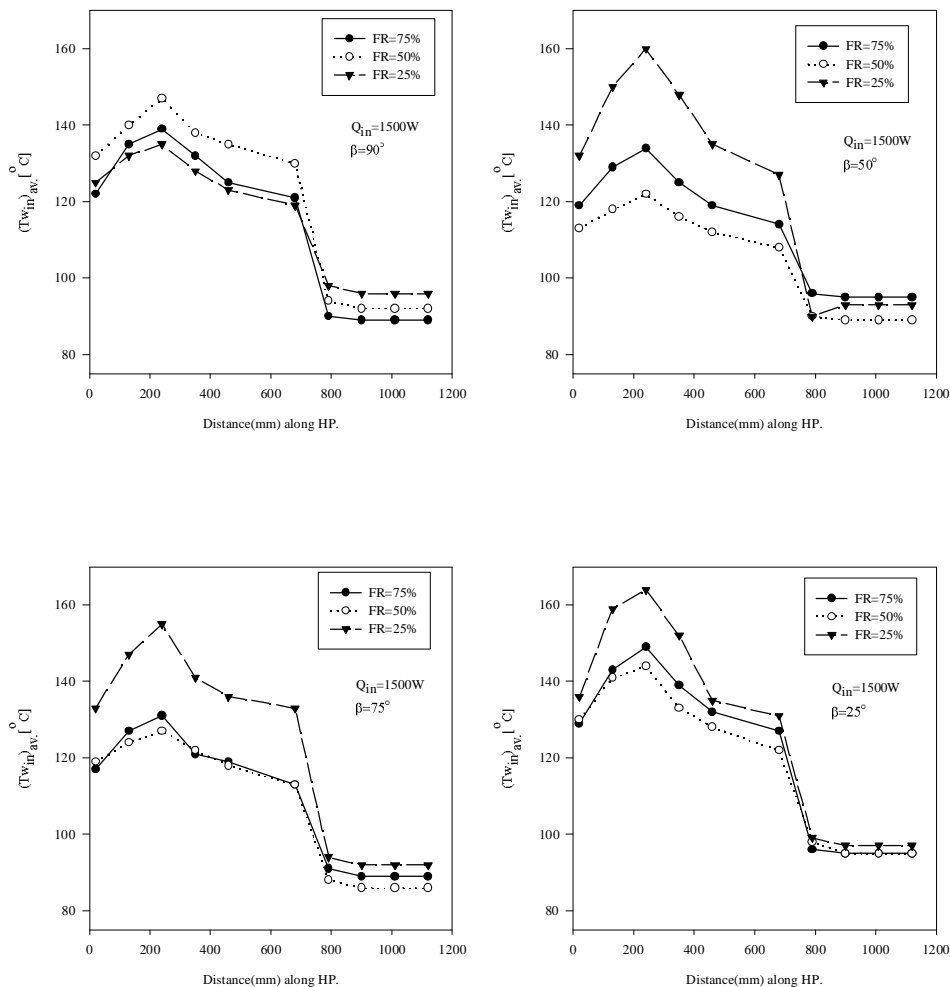
Figure(3):Variation of average wall temperature along the HP at different water filling ratios for different inclination angles.

Figure(4):Variation of average wall temperature along the HP at different water filling ratios for different powers.
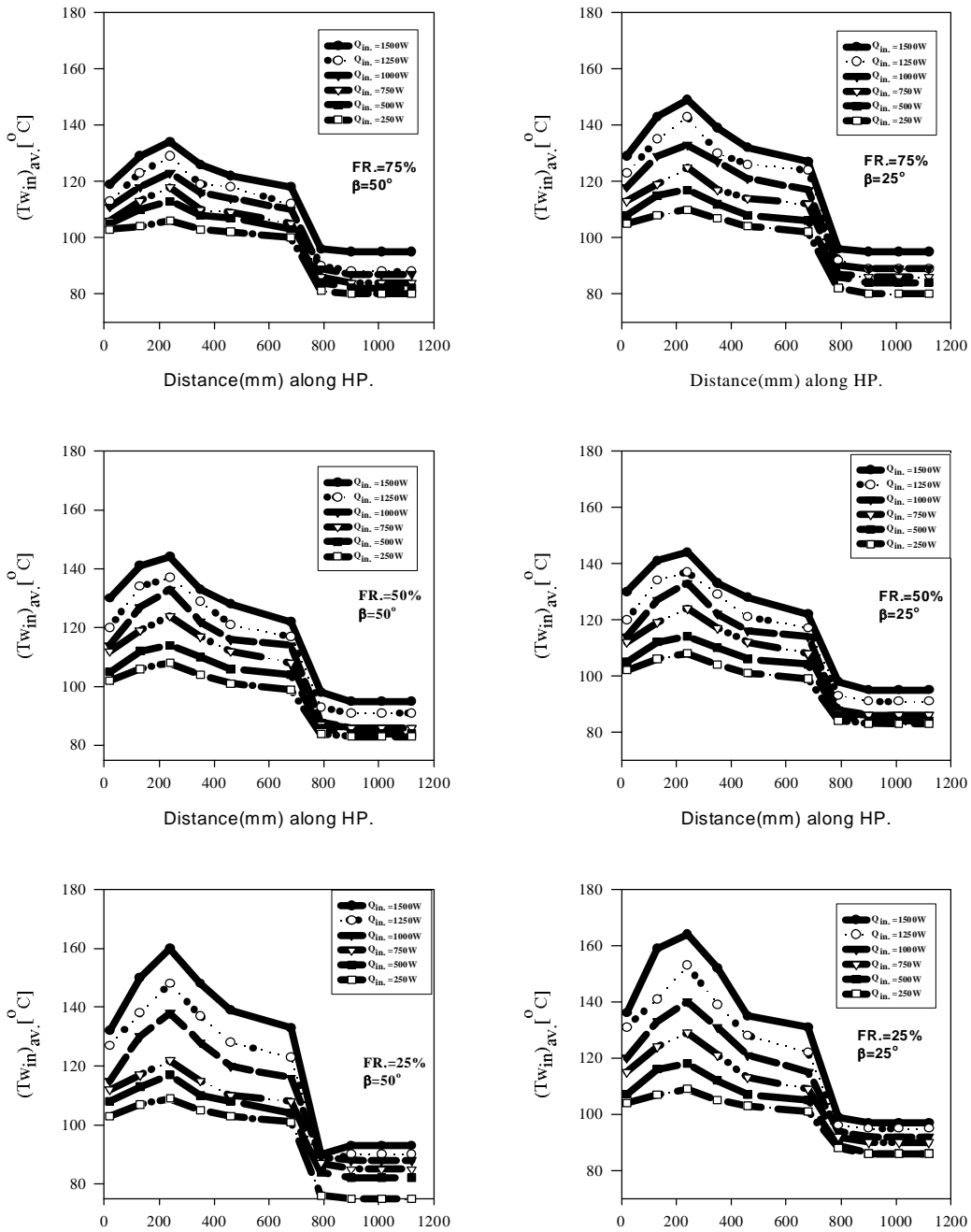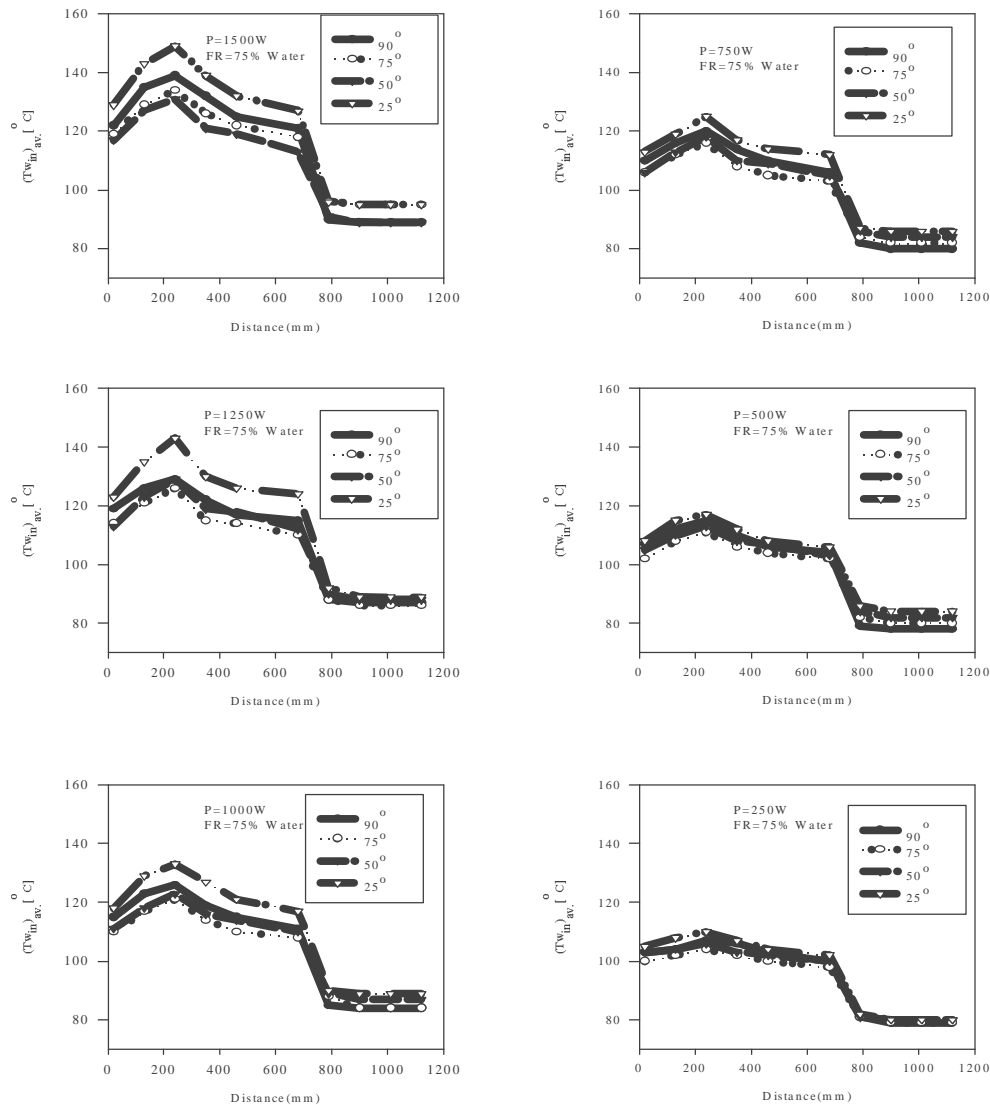
Figure(5):Variation of average wall temperature along the HP at different water filling ratios for different powers.
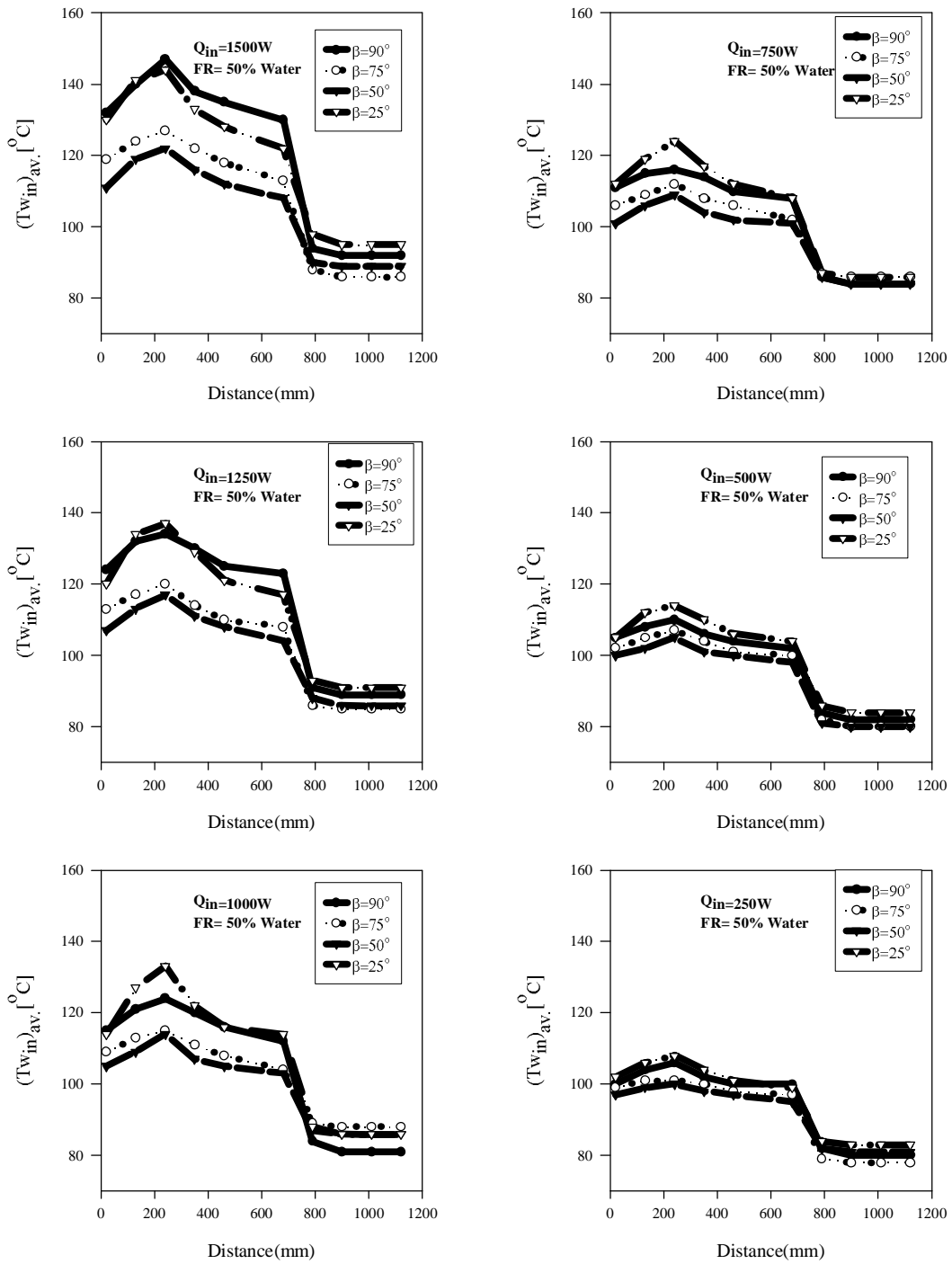
4.4: Effect of the Inclination Angle

The heat transfer by boiling in the evaporator section shows larger local differences and depends on inclination. The intention here to gain better insight into the transport processes of HP by observing local phenomena in different parts of the device. especially the effects of the

inclination of HP. This behavior is observed in the experimental HP as shown in figures (6) and (7) show the temperature against the distance along HP for (75%and50%) filling ratios. Thus, they show that the temperature of the evaporator is higher when the inclination angle(β) is $25^o$and decreases when β equals $50^o$and 75°, and starts to increase when the angle becomes 90°. While for the filling ratio 25%, figure(8) the temperature decreases as the inclination angle increases from 25° to 90°. As the angle of inclination further decreases (i.e. as the heat pipe approaches the horizontal position) then plug flow boiling dominates the entire region of the evaporator. Boiling changes from nucleate boiling (in the liquid film region and the submerged region at vertical position)to nucleate boiling (in wetted region and dry region).

Figure(6): Variation of average wall temperature along the HP at different inclination angles and power input.

Figure(7):Variation of average wall temperature along the HP at different inclination angles and power input.
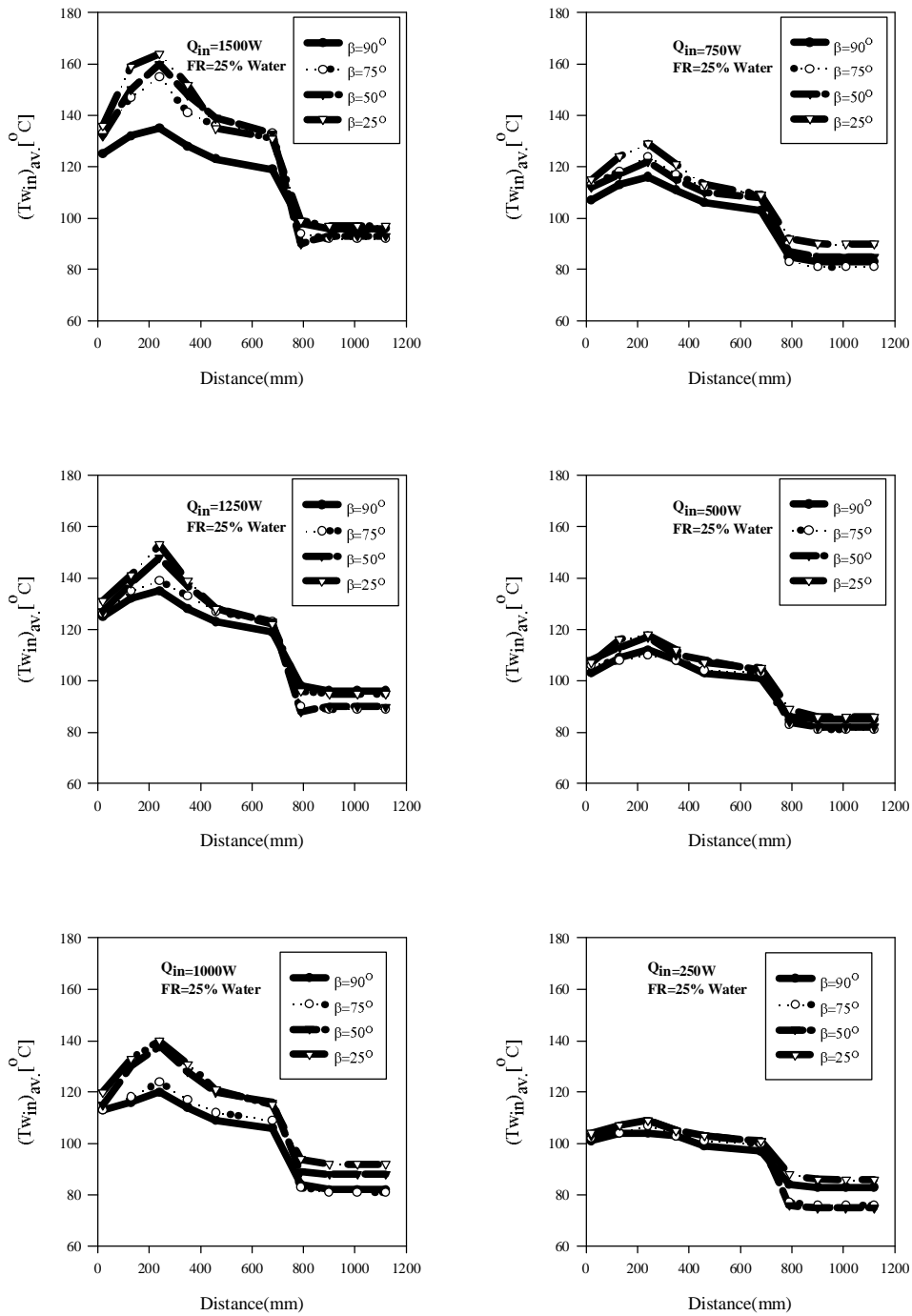
Figure(8):Variation of average wall temperature along the HP at different inclination angles and power input.

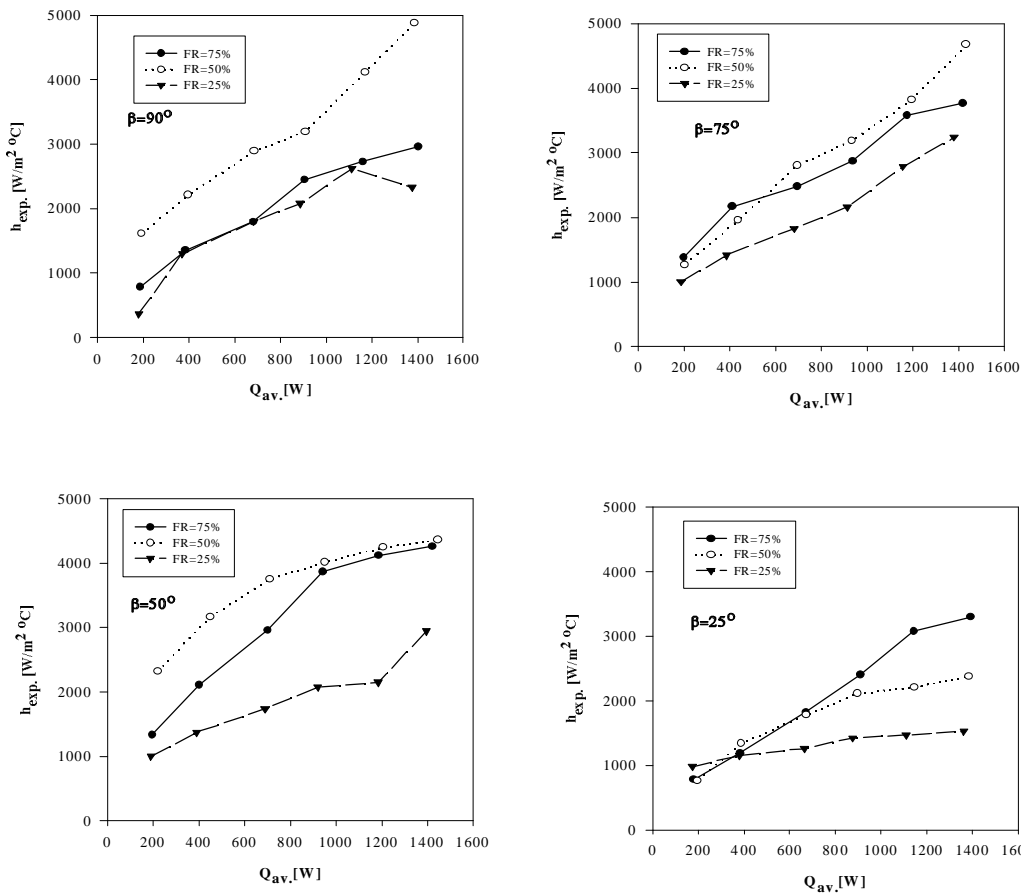### 4.5: Effects of Filling Ratio on the Heat Transfer Coefficient

Figure(9) represents the average heat ($Q_{av.}$) against the heat transfer coefficient for different filling ratio charges at a given inclination angle. The heat transfer coefficient (h_{exp}) can be calculated by using the following correlation[7,15]:

$$h_{exp.} = \frac{Qav.}{\pi \cdot D_i \cdot l_e \cdot (T_w - T_{v.})} \tag{8}$$

Where;

$$Q_{av} = \frac{Q_{in} + Q_o}{2}$$

The large value of the heat transfer coefficient, which can be seen from figures, is at 50% charge, for all power inputs at angles(90°, 75° and 50°).While when the HP was tilted by an angle 25°, as shown, the higher values of heat transfer coefficient are at75% filling ratio. As the HP inclines towards the horizontal level ($\beta=25^o$) the heat transfer coefficient increases with the increase of the filling ratio due to the increase of the heat transfer area between the wall and the working fluid. For other inclination angles (50° , 75° and 90°), the maximum heat transfer area found to be at 50% filling ratio.
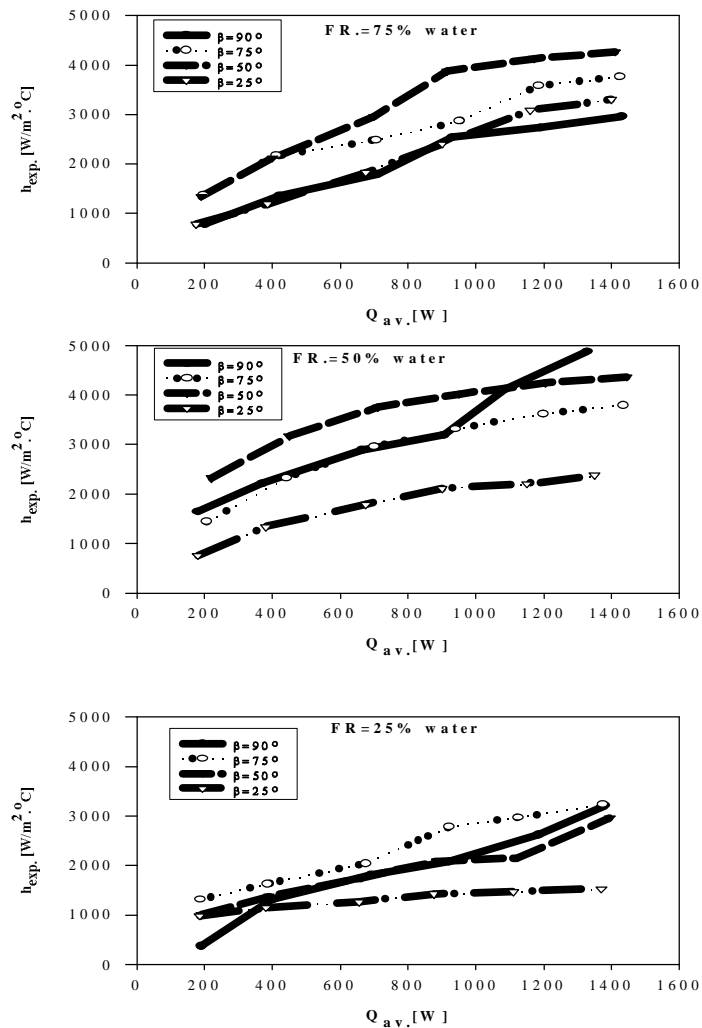

Figure(9):Heat transfer coefficient vs. the average heat input with different filling ratio and different inclination angles.

4.6: Effect of Inclination Angle on the Heat Transfer Coefficient

Figure(10)shows that the maximum heat transfer coefficient was obtained when the inclination angle is 50° and the filling ratio is 50% and 75%, while the maximum heat transfer coefficient at 25% filling ratio is when the HP is at vertical position. The minimum heat transfer coefficient occurs when the inclination angle is 75° and the filling ratio is 25%.

In general the highest heat transfer coefficient for all experimental tests was found at the inclination angle 50° and the filling ratio 50%.

As the HP tilted towards the horizontal position the heat transfer decreases because of the accumulation of bubbles on the inside upper surface of the evaporator due to the buoyancy forces. On the other side when the HP approaches 50° inclination angle, the effect of the buoyancy force seems to be vanished and the maximum heat transfer coefficient decreases.

Figure(10):Heat transfer   coefficient vs. the average heat input at different filling ratios for different inclination angles.

113

5: Comparison of the Experimental Results with the Theoretical and Empirical Correlations

The experimental heat transfer coefficients of the present work calculated by Equation (8) were compared with that predicted by Rohsenow and Imura in Equations (9)and (10) respectively is illustrated in Figure (11) for tilt angle 90° and (25%,50% and 75%). It is clear from the figure that the experimental results of heat transfer coefficient are well agreed with that calculated by the theoretical (Rohsenow) and empirical (Imura) correlations specially when the filling ratio is 50% .
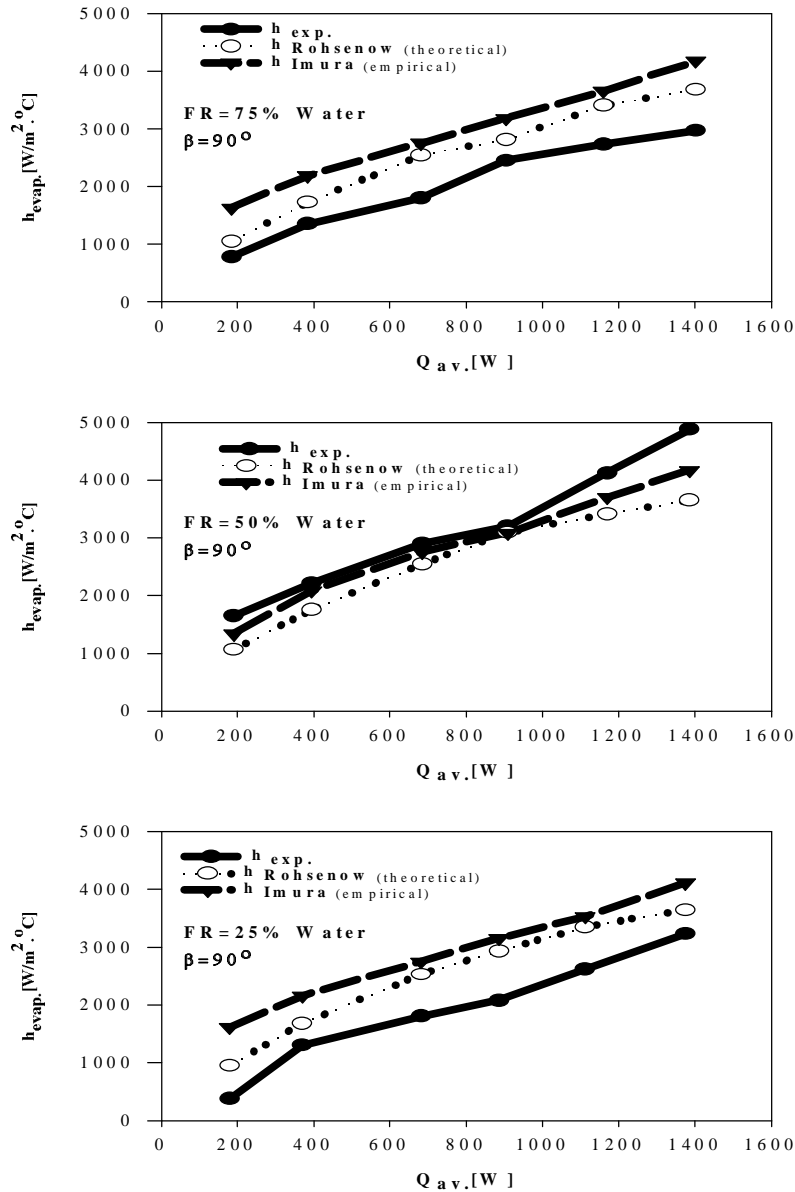
Figure(11):Heat transfer coefficient vs. with average heat input compared with theoretical and empirical correlations for different filling ratios.

$$h_{Rohsenow} = \frac{q_e^{2/3}}{\frac{C_{sf} \times h_{fg}}{C_{p,l}} \cdot \left\{ \frac{1}{h_{fg} \times \mu_l} \left[\frac{\sigma_l}{g \cdot (\rho_l - \rho_v)} \right]^{0.5} \right\}^{1/3} \cdot P_r^{1.7}} \qquad (9)$$

$$h_{Imura} = 0.32 \cdot \frac{\rho_l^{0.65} \cdot k_l^{0.3} \cdot C_{p_l}^{0.7} \cdot g^{0.2} \cdot q_e^{0.4}}{\rho_v^{0.25} \cdot h_{fg}^{0.4} \cdot \mu_l^{0.1}} \left[\frac{P_{v.}}{P_{atm.}} \right]^{0.3} \qquad (10)$$

6: Conclusions

From the present work, the following conclusions can be extracted:

1-The temperature distribution along the HP wall in the evaporator section is almost isothermal. The measured temperature along the condenser showed lower values. This drop of temperature is expected because of the internal resistances due to boiling and condensation.

2- For all heat inputs it was found that the average outside temperature of evaporator section is low when the filling ratio is 50% and the inclination angle is 50°.

3-The experimental results indicate that the filling ratio and the heat input have the important effects on the heat transfer performance. The optimal performance of the HP was found when the filling ratio ranged between 50–75%, at 50° inclination angle, while the minimum performance was found when the filling ratio was 25% and 25° inclination angle.

4- Maximum thermal conductivity of the HP was found to be about 2060 times that of a stainless steel piece of the same size.

5-The experimental heat transfer coefficient results agreed well with the empirical and mathematical models for HP.

REFERENCES

1. Yahya, A. A., "Design and Development of An Indirect Type of Solar Cooker Using a Heat Pipe," M.Sc. Thesis, Mosul University, College of Engineering ,(1980).
2. Frank M., "Improving Injection Lances With Heat Pipe Technology," McGill University, (2000)
3. Kempers, R., Ewing,D. and Ching,C.Y.,"Effect of Number of Mesh Layers and Fluid Loading of Screen Mesh Wicked Heat Pipe," Journal of Applied Thermal Engineering, (2006).
4. Jianlin Yu, Hua Chen, Hua Zhoa, and Yanzhong Li, "An Experimental   Investigation on Capillary Pumped Loop With the Meshes Wick," International Journal of Heat and Mass Transfer 50 (2007) 4503–4507.
5. Shwin-Chung Wong and Yi-Huan Kao, "Visualization and Performance Measurement of Operating Mesh-wicked Heat Pipes," International Journal of Heat and Mass Transfer (2008).
6. Reay, D.A. and Kew ,p.," Heat Pipes Theory, Design and Applications,"5[rd.] Edition, Britain,(2006).

7. Noie, S.H., "Heat Transfer Characteristics of a Two-phase Closed Thermosyphon," Journal of Applied Thermal Engineering 25(2005) 495–506.

8. Shiraish, M., Kikuchi, K. and Yamanishi,T., "Investigation of Heat Transfer Characteristics of a Two-phase Closed Thermosyphon," Japane(1981).

9. Bejan, A. and Kraus A.D., "Heat Transfer Handbook," Published by John Wiley & Sons, Inc., Hoboken, New Jersey,(2003).

10. Peterson, G.P. ,"An Introduction to Heat Pipes Modeling, Testing and Applications," Newyork,(1994).

11. Sumana, B., "Design of Heat Pipe," Thesis, Indian Institute of Technology, MAY (2003).

12. Ninad D. Sathayea "Incorporation of Heat Pipe into Engine air Pre-cooling Study," M.Sc. Thesis, B. E., University of Pune,2000. Kansas state university Manhattan, Kansas(2003).

13. Reay, D.A., "Advances in Heat Pipe Technology", Pergammon,1981.

14. Kreith,F.,Boehm,R.F.,Raithby,G.D. and Hollands,K.G., "Heat and Mass   Transfer Handbook, " CRC Press LLC,(2000).

15. Kreith, F., "Principles of Heat Transfer,"3rd Edition, Interstate Educational Publishers, U.S.A. (1997).